FEBS Letters 353 (1994) 273–276

FEBS 14660

Asymmetric binding of the primary acceptor quinone in reaction centers of the photosynthetic bacterium *Rhodobacter sphaeroides* R26, probed with Q-band (35 GHz) EPR spectroscopy

Johan S. van den Brink[a], Andrej P. Spoyalov[b], Peter Gast[a], Willem B.S. van Liemt[c], Jan Raap[c], Johan Lugtenburg[c], Arnold J. Hoff[a,*]

[a]*Department of Biophysics, Huygens Laboratory, Leiden University, P.O. Box 9504, 2300 RA Leiden, The Netherlands*
[b]*Institute of Chemical Kinetics and Combustion, Russian Academy of Sciences, Novosibirsk, 630090, Russian Federation*
[c]*Leiden Institute of Chemistry, Gorleaus Laboratories, Leiden University, P.O. Box 9502, 2300 RA Leiden, The Netherlands*

Received 27 July 1994; revised version received 8 September 1994

Abstract The reaction center (RC)-bound primary acceptor quinone Q_A of the photosynthetic bacterium *Rhodobacter sphaeroides* R26 functions as a one-electron gate. The radical anion $Q_A^{\bullet-}$ is proposed to have an asymmetric electron distribution, induced by the protein environment. We replace the native ubiquinone-10 (UQ10) with specifically ^{13}C-labelled UQ10, and use Q-band (35 GHz) EPR spectroscopy to investigate this phenomenon in closer detail. The *direct* observation of the ^{13}C-hyperfine splitting of the g_z-component of $UQ10_A^{\bullet-}$ in the RC and in frozen isopropanol shows that the electron spin distribution is symmetric in the isopropanol glass, and asymmetric in the RC. Our results allow qualitative assessment of the spin and charge distribution for $Q_A^{\bullet-}$ in the RC. The carbonyl oxygen of the semiquinone anion nearest to the S = 2 Fe^{2+}-ion and Q_B is shown to acquire the highest (negative) charge density.

Key words: Reaction center; Quinone; EPR; ^{13}C-hyperfine coupling; Photosynthesis; *Rhodobacter sphaeroides* R26

1. Introduction

Quinones act as electron acceptors in primary photosynthetic electron transport. They are embedded in a protein–pigment complex, the so-called reaction center (RC), which contains two functionally distinct quinones, one of which (Q_A) acts as a one-electron gate, passing the electron to a second quinone, Q_B, which accepts two electrons and two protons. Where Q_BH_2 exchanges with the membrane-bound quinone pool, Q_A is tightly bound to the RC. In the RC of the photosynthetic purple bacterium *Rb. sphaeroides* R26, *both* quinones are ubiquinone-10 (UQ-10) molecules (see Fig. 1 for the chemical structure and nomenclature). Consequently, the functional difference between Q_A and Q_B must be related to a different interaction with the protein environment.

^1H-ENDOR spectroscopy first revealed such a difference for $Q_A^{\bullet-}$ and $Q_B^{\bullet-}$. The spectral features of $Q_B^{\bullet-}$ were shown to be much more similar to the radical anion of UQ-10 in frozen isopropanol than $Q_A^{\bullet-}$ [1,2]. An inequivalence of the hydrogen bonds to the two carbonyl oxygens of Q_A was proposed from the crystal structure [3], which may be related to an asymmetric electron spin density distribution in $Q_A^{\bullet-}$, as distinct from the situation in isopropanol glass, where the electron spin density is (nearly) symmetrically distributed over the molecule [4]. Proton ENDOR of the methyl group of $Q_A^{\bullet-}$, however, provides only indirect information on the carbon spin densities. ^{17}O-EPR results showed that both carbonyl oxygens are inequivalent for $Q_A^{\bullet-}$, but no assignment could be made which of the carbonyls possesses the highest charge-density. Recently, UQ-10 specifically ^{13}C-labelled at positions 1, 2, 3, 3^1, and 4 has been prepared [5]. ^{13}C-MAS-NMR spectroscopy of quinone-reconstituted RCs of *Rb. sphaeroides* R26 revealed that the carbonyl carbon atoms (1 and 4) are inequivalent for the ground state of Q_A [6]. FTIR reduced–unreduced difference spectroscopy of uniformly ^{13}C-labelled quinone containing RCs showed that the bonding strength of the two carbonyls is inequivalent also for $Q_A^{\bullet-}$ [7], but no *unambiguous* assignment could be made for the resonances, due to admixture of the C = C stretch vibrations in the C = O stretch vibrations. A spectroscopic technique that probes with *atomic selectivity* details on the spin- and charge-distribution of $Q_A^{\bullet-}$ not available with any other spectroscopy, is EPR of specifically ^{13}C-enriched quinones.

In this communication, we use Q-band (35 GHz) EPR spectroscopy to study the UQ-10 radical anion in the RC ($Q_A^{\bullet-}$) and in frozen isopropanol to obtain more direct information on the (a)symmetry of the electron distribution of $Q_A^{\bullet-}$. Observation of the ^{13}C-hyperfine splitting of the g_z-peak in the quinone Q-band spectrum allows unequivocal experimental confirmation that the charge- and spin-distribution is asymmetric for $Q_A^{\bullet-}$ [1,2]. From the measured ^{13}C-hyperfine tensor elements, we conclude that the electron spin density on the even-numbered carbons *increases* and for the odd-numbered carbons *decreases* for $Q_A^{\bullet-}$ relative to the ubiquinone radical anion in isopropanol glass. Therefore, the carbonyl oxygen at position 4 is more electronegative than its counterpart at position 1, which property may facilitate electron transport from $Q_A^{\bullet-}$ to Q_B.

*Corresponding author. Fax: (31) (71) 275 819.

Abbreviations: RC, reaction center; *Rb.*, *Rhodobacter*; Q_A, primary acceptor quinone; Q_B, secondary acceptor quinone; UQ, ubiquinone; MAS, magic angle spinning; FTIR, Fourier-transform infra-red; ENDOR, electron-nuclear double resonance; EPR, electron paramagnetic resonance; ESP, electron spin polarisation.

2. Materials and methods

Specifically ^{13}C-enriched quinones were synthesised as described [5]. RCs of *Rb. sphaeroides* R26 were isolated according to [8]. Removal of Q_B and Q_A, and reconstitution of Q_A with the ^{13}C-labelled UQ10, was

SSDI 0014-5793(94)01047-1

performed according to [9]. The yield of the procedures, checked with room-temperature ΔA_{865} measurements, was better than 90% for (Q_A,Q_B)-removal and Q_A-reconstitution. The Q_B-content of the reconstituted RCs was less than 5%, as determined from room-temperature rereduction of P^{+}.

For the EPR measurements, the native S = $2Fe^{2+}$-ion, which forms a magnetically coupled complex with $Q_A^{\bullet-}$ [10], was replaced with diamagnetic Zn^{2+}. For this purpose, the LDAO (*N*,*N*-dimethyldodecylamine-*N*-oxide, Fluka) of the RC stock solution was replaced by Brij 58 (polyoxyethylene-20-cetyl-ether, Sigma) using precipitation with BioBeads SM-2 [11]. Subsequently, the Fe^{2+}-ion was removed [12], and replaced by Zn^{2+} [13]. A typical EPR sample contained about 60% (v/v) glycerol, yielding an optically transparant glass. The final RC concentration was about 50 μM.

Quinone anion radicals were created in anoxic isopropanol by reduction with potassium *tert*-butyrate. The isopropanol forms a good glass, so that the micro-environment of all radicals is comparable.

EPR experiments were performed on our home-built superheterodyne Q-band (34.8 GHz) EPR spectrometer, which we modified from the original set-up described in [14]. The superheterodyne set-up allows high-sensitivity, low-noise detection, and can be operated at very low incident microwave powers (down to 1 nW). Briefly, the spectrometer consists of two oscillators locked at a difference frequency of 60.005 MHz. The main oscillator (MO) is a low-noise 60 mW Varian 35 GHz VA284B klystron, with 1 GHz mechanical, and 100 MHz electronic tuning range. The local oscillator (LO) is a voltage-controlled Alpha Industries (CME 713AH) 35 GHz gunn oscillator with 250 MHz mechanical, and 100 MHz electronic tuning range. The spectrometer is equipped with a cylindrical TE011 cavity, whose resonance frequency is phase-locked with the frequency of the MO. Top-loading of the cavity allows for easy sample exchange. A stable magnetic field up to 1.50 T is provided by a Bruker water-cooled electromagnet. The magnetic field-modulation frequency is low (73 Hz), and the EPR signal is detected from the rectified 60 MHz signal using an EG&G lock-in amplifier and ADC. Spectra are recorded using an IBM-compatible computer. All measurements were performed in a home-built bath crysostat filled with cold N_2 gas ($T \approx 100$ K).

Simulations of the powder spectra were performed with the EPR simulation program developed by J.A. Weil and co-workers [15,16], running on a Personal IRIS workstation.

3. Results and discussion

The Q-band EPR spectrum of unlabelled $Q_A^{\bullet-}$ in RCs of *Rb. sphaeroides* R26 was first reported in [17]. Fig. 2A shows the corresponding spectrum for our RCs (solid line), together with a simulated lineshape (dashed line) using the *g*-tensor of $Q_A^{\bullet-}$ from [18] and anisotropic line-broadening ΔW mimicking unresolved hyperfine splittings. The relative magnitudes of the linewidth components ($\Delta W_Y/\Delta W_Z = 1.7$) are comparable with those in [18] ($\Delta W_Y/\Delta W_Z = 1.5$), but the absolute amplitude is smaller at Q-band than at W-band (95 GHz), as expected [19,20]. The principal *g*-tensor elements and the corresponding ΔW-values at Q-band are shown in Table 1. Using these values, we simulated all spectra for the specifically ^{13}C-enriched quinone anion radicals. The *z*-directions of the ^{13}C-hyperfine tensors (A^C) and the *g*-tensor are collinear for the carbon atoms of π-radicals, and coincide with the normal of the plane of the molecule [21–23]. The *x*-direction of the *g*-tensor is the axis connecting the carbonyl oxygens, which is collinear with the

Table 1
Diagonal elements of the *g*-tensor [18] and the anisotropic line-broadening tensor ΔW for $Q_A^{\bullet-}$ in RCs of *Rb. sphaeroides* R26

	X	Y	Z
g	2.0066	2.0056	2.0022
ΔW (mT)	0.56	0.80	0.45

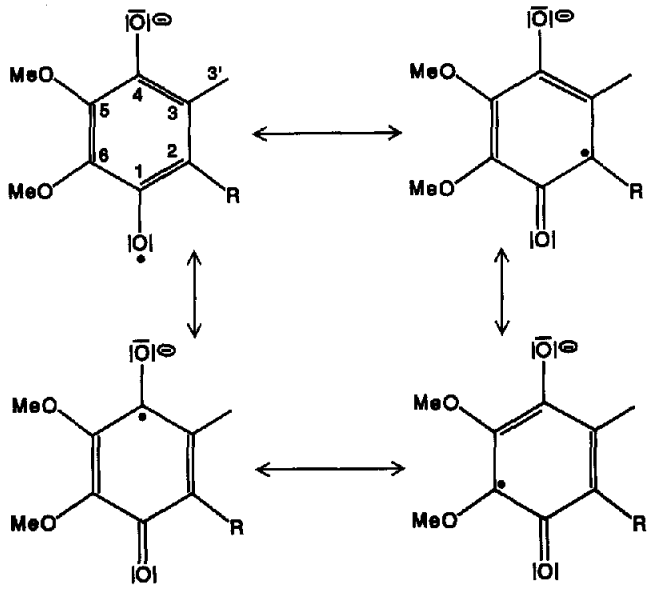

Fig. 1. Chemical structure and nomenclature of the radical anion of ubiquinone-10. R denotes the side chain consisting of (in this case) 10 isoprenoid subunits. Also shown are the Kékulé resonance structures for $Q_A^{\bullet-}$ in the RC, where the free electron is asymmetrically delocalised (see text). It is seen that in this case the free electron is mainly localised on $C_{2,4,6}$ and O_1 of $Q_A^{\bullet-}$, whereas the partial-negative charges reside on the complementary atoms (Kékulé resonances not shown).

x-component of A^C for the carbonyl carbon atoms. For the other carbons, the *x*-axis points in the direction of the substituent, thus making an angle of about 60° with g_x.

Figs. 2B–F show the Q-band EPR spectra (solid lines) and simulations (dashed lines) for RCs reconstituted with the specifically ^{13}C-enriched quinones. The ^{13}C-hyperfine parameters (absolute values) used for the spectral simulations are summarised in Table 2. The spectra for 3-^{13}C and 3^1-^{13}C closely resemble that of the unlabelled quinone, indicating that $|A^C_{x,y,z}| < 0.25$ mT (simulations not shown). The low-field features (unresolved g_x and g_y lines) for 2-^{13}C and 4-^{13}C are not visibly broadened with respect to those of unlabelled $Q_A^{\bullet-}$, so that for these positions $|A^C_{x,y}| < 0.25$ mT. The simulations yield $|A^C_z| = 0.55 \pm 0.03$ mT and 1.27 ± 0.03 mT for 2-^{13}C and 4-^{13}C, respectively. The spectrum for 1-^{13}C $Q_A^{\bullet-}$ not only shows a clear splitting of the g_z-feature, but also a broadening of the low-field features. Spectral simulations show that the ^{13}C-hyperfine tensor is nearly isotropic in this case, with $|A^C_x| = 0.55 \pm 0.05$ mT, $|A^C_y| = 0.65 \pm 0.05$ mT, and $|A^C_z| = 0.80 \pm 0.03$ mT. Here, all three tensor components have the same sign (either positive or negative). The small anisotropy of A^C for 1-^{13}C in $Q_A^{\bullet-}$ is caused by the low electron spin density on this atom [23,24].

Because the Q-band spectra for 1-^{13}C and 4-^{13}C, and for 2-^{13}C and 3-^{13}C UQ-10, in the Q_A-binding pocket of the RC of *Rb. sphaeroides* R26 are clearly different, we conclude that the electron spin is distributed asymmetrically over the respective C-atoms. This contrasts with the situation in a frozen solution of isopropanol, where the electron spin densities are comparable for the respective atoms of the quinone anion radical [4]. Since ^{13}C-hyperfine couplings for carbonyl functions are very sensitive to the polarisability of the C and the O atoms, we determined $|A^C_z|$ for 1-^{13}C (Fig. 3A) and 4-^{13}C (Fig. 3C) for UQ-10 anion radicals in frozen isopropanol. Isopropanol forms

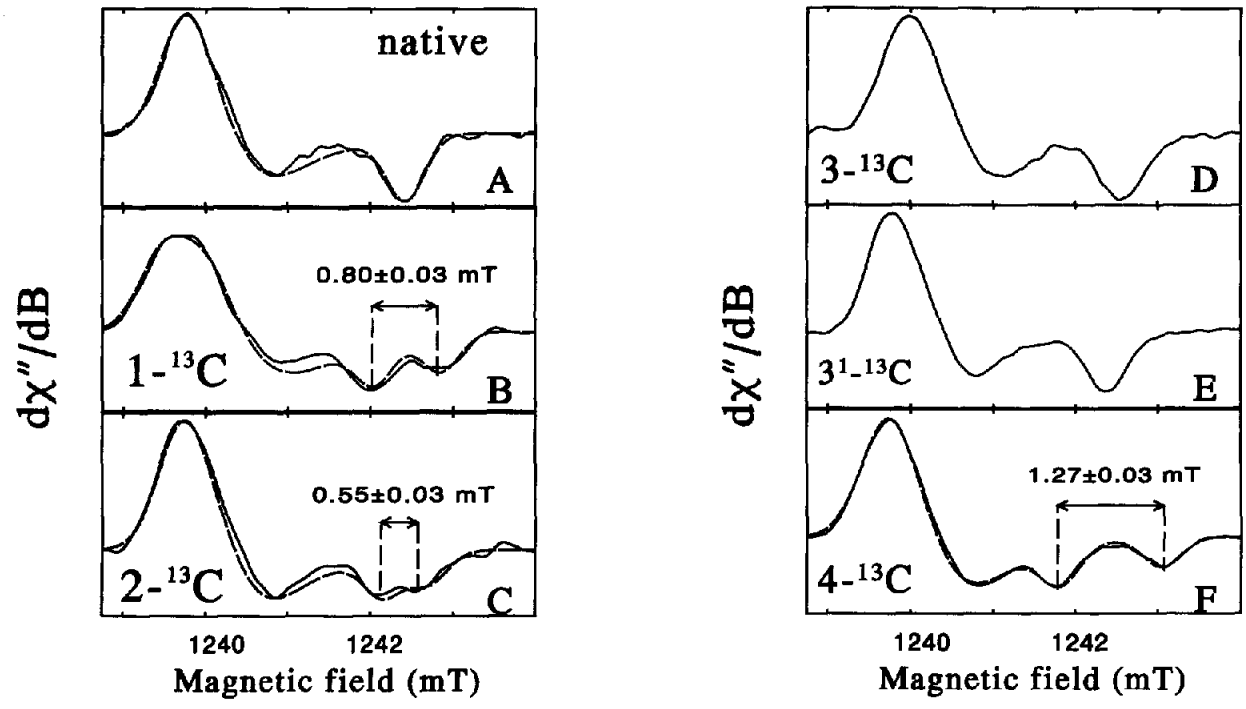

Fig. 2. Q-band EPR spectra of the primary acceptor quinone radical anion in RCs of *Rb. sphaeroides* R26. A, unlabelled; B, 1-^{13}C-labelled; C, 2-^{13}C-labelled; D, 3-^{13}C-labelled; E, 3^{1}-^{13}C-labelled; and F, 4-^{13}C-labelled ubiquinone-10. Experimental conditions: microwave frequency, 34,803 GHz; microwave power, 50 nW; temperature, 100 K; magnetic field-modulation amplitude, 0.20 mT; scan time, 600 s; time constant, 3 s.

a good glassy matrix in which the carbonyls of the quinone are expected to make hydrogen bonds of equal strength. Fig. 3 shows the experimental spectra, from which we determined that $|A_z^C| = 1.13 \pm 0.03$ mT for 1-^{13}C, and 1.10 ± 0.03 mT for 4-^{13}C, respectively, showing the equivalence of 1-^{13}C and 4-^{13}C. Furthermore, Fig. 3B shows the Q-band EPR spectrum for the radical anion of 2-^{13}C UQ-10, in which no splitting of the g_z-peak is observed. The line is broadened, however, compared to that of 3^{1}-^{13}C (Fig. 2E), which yields $|A_z^C| \approx 0.40$ mT.

Accurate spin densities can be calculated when both the isotropic *and* the dipolar part of the ^{13}C-hyperfine tensor (including signs) are known [25,26]. The dipolar part gives the spin density in the π-orbital, whereas the isotropic part is sensitive to spin density in the s-orbitals *and* to spin polarisation contributions due to neighbouring atoms. For example, using the spin densities from [4], the z-component of the dipolar part of the hyperfine tensor is 1.17 mT. The Karplus–Fraenkel theory yields $A_{iso} = -0.04$ mT, which implies $A_z^C = 1.13$ mT, in close agreement with the experimental results for $UQ10^{\bullet-}$ in isopropanol glass.

Since we know for most carbon positions of $Q_A^{\bullet-}$ only the magnitude of A_z^C, we are not yet able to calculate definitively the spin densities for all carbon positions. Work is in progress to determine all the necessary parameters, using ENDOR, ESEEM, and time-resolved EPR spectroscopy of the radical pair $P^{\bullet+}Q_A^{\bullet-}$ (see e.g. [27–29]). In spite of the lack of detailed information on the dipolar hyperfine coupling, the present data allows to draw a few tentative conclusions. For example, because $|A_C|$ of 1-^{13}C is largely isotropic, the electron spin density on this atom must be relatively low [23,24]. The increased value of $|A_z^C|$ for 2-^{13}C and 4-^{13}C of $Q_A^{\bullet-}$ compared to the UQ-10 anion radical in frozen isopropanol, indicates that the electron spin density on this carbon atom is somewhat larger in the RC than in frozen isopropanol. (Using the maximum and minimum values for the z-component of the dipolar hyperfine tensor, we estimate: $0.11 < \rho_4 < 0.16$, and $0.03 < \rho_2 < 0.08$). This data indicates that the spin-density distribution is distorted in the RC, with relatively high spin density on $C_{2,4,6}$ and O_1, as can be seen from the Kékulé resonance structures in Fig. 1. The charge is then mainly located on the complementary part of the molecule. We can now also assign the inequivalence observed from ^{17}O-EPR [2] to be related to relatively higher electron spin density on O_1. Consequently, O_4 is more electronegative than O_1, which immediately relates to the reported stronger hydrogen bonding of O_4 with the protein residue (most likely with His M219 [3]) as compared with O_1. O_4 is the oxygen nearest to the divalent metal ion, which is also coordinated with His M219 [3]. The asymmetric charge distribution, with excess partial negative charge on O_4, presumably facilitates electron transport from Q_A to Q_B. Whether this asymmetric spin-density distribution in the quinone is an instanteneous process, or is due to an increase of hydrogen-bonding strength, possibly related to reported light-induced changes of the $P^{\bullet}Q_A^{\bullet-}$ radical pair [30,31], will be investigated with ESP spectroscopy.

Table 2
Principal ^{13}C-hyperfine tensor elements (in mT) for $Q_A^{\bullet-}$ in RCs of *Rb. sphaeroides* R26, determined from simulations of experimental Q-band (35 GHz) EPR spectra.

	$\|A_x^C\|$	$\|A_y^C\|$	$\|A_z^C\|$
1–^{13}C	0.55 ± 0.05	0.65 ± 0.05	0.80 ± 0.03
2–^{13}C	< 0.25	< 0.25	0.55 ± 0.03
3–^{13}C	< 0.25	< 0.25	< 0.25
3^{1}–^{13}C	< 0.25	< 0.25	< 0.25
4–^{13}C	< 0.25	< 0.25	1.27 ± 0.03

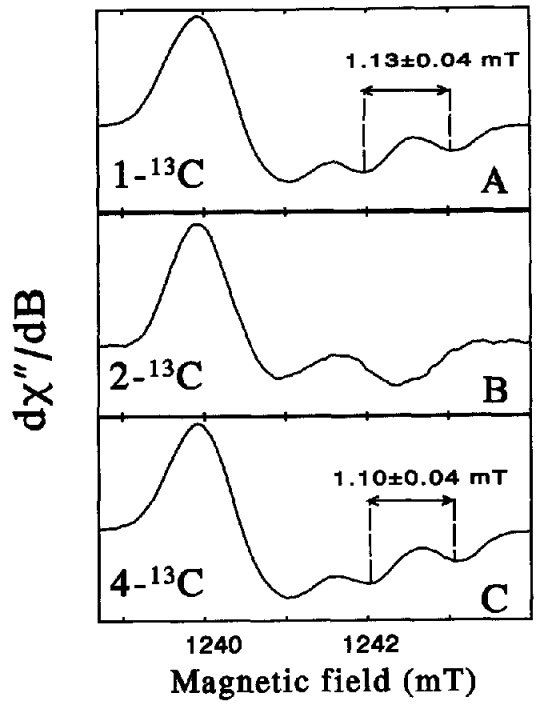

Fig. 3. Q-band EPR spectra of the radical anion of ubiquinone-10 in frozen isopropanol. A, 1-^{13}C; B, 2-^{13}C; C, 4-^{13}C ubiquinone-10. Experimental conditions: microwave frequency, 34.803 GHz; microwave power, 50 nW; temperature, 100 K; magnetic field-modulation amplitude, 0.20 mT; scan time, 600 s; time constant, 3 s.

Acknowledgements: We thank Drs. H. Manikowski (Technical University, Poznan, Poland) and I.I. Proskuryakov (Academy of Sciences, Pushchino, Russia) for their help with improving the Q-band spectrometer, Mr. A.H.M. de Wit for growing the bacteria, and Ms. S.J. Jansen for help with preparing the RCs. This research was supported by the Netherlands Foundation for Chemical Research (SON), financed by the Netherlands Organisation for Scientific Research (NWO). A.S. acknowledges a travel grant of the Netherlands Organisation for Scientific Research (NWO). P.G. is a research fellow of the Royal Netherlands Academy of Arts and Sciences (KNAW).

References

[1] Lubitz, W., Abresch, E.C., Debus, R.J., Isaacson, R.A., Okamura, M.Y. and Feher, G. (1985) Biochim. Biophys. Acta 808, 464–469.
[2] Feher, G., Isaacson, R.A., Okamura, M.Y. and Lubitz, W. (1985) in: Antennas and Reaction Centers of Photosynthetic Bacteria (Michel-Beyerle, M.E., Ed.) pp.174–189, Springer, Berlin.
[3] Allen, J.P., Feher, G., Yeates, T.O., Komiya, H. and Rees, D.C. (1988) Proc. Natl. Acad. Sci. USA 85, 8487–8491.
[4] Das, M.R. and Fraenkel, G.K. (1963) J. Chem. Phys. 42, 1350–1360.
[5] Van Liemt, W.B.S., Steggerda, W.F., Esmeijer, R. and Lugtenburg, J. (1994) Recl. Trav. Chim. Pays-Bas 113, 153–161.
[6] Van Liemt, W.B.S., Boender, G.J., Gast, P., Hoff, A.J., Lugtenburg, J. and De Groot, H.J.M. (1993) Photochem. Photobiol. 57, 32S.
[7] Breton, J., Burie, J.-R., Berthomieu, C., Berger, G. and Nabedryk, E. (1994) Biochemistry 33, 4953–4965.
[8] Feher, G. and Okamura, M.Y. (1978) in: The Photosynthetic Bacteria (Clayton, R.K. and Sistrom, W.R., Eds.) pp. 349–386, Plenum Press, New York.
[9] Okamura, M.Y., Isaacson, R.A. and Feher, G. (1975) Proc. Natl. Acad. Sci. USA 72, 3491–3495.
[10] Butler, W.F., Calvo, R., Fredkin, D.R., Isaacson, R.A., Okamura, M.Y. and Feher, G. (1984) Biophys. J. 45, 947–973.
[11] Gast, P., Hemelrijk, P. and Hoff, A.J. (1994) FEBS Lett. 337, 39–42.
[12] Tiede, D.M. and Dutton, P.L. (1981) Biochim. Biophys. Acta 637, 278–290.
[13] Debus, R.J., Feher, G. and Okamura, M.Y. (1986) Biochemistry 25, 2276–2287.
[14] Brok, M. (1985) Thesis Leiden University.
[15] Weil, J.A. (1971) J. Magn. Res. 4, 394–399.
[16] Mombourquette, M.J. and Weil, J.A. (1992) J. Magn. Res. 99, 37–44.
[17] Feher, G., Okamura, M.Y. and McElroy, J.D. (1972) Biochim. Biophys. Acta 267, 222–226.
[18] Burghaus, O., Plato, M., Rohrer, M., Möbius, K., McMilland, F. and Lubitz, W. (1993) J. Phys. Chem. 97, 7639–7647.
[19] Prisner, T.F., McDermott, A.E., Un, S., Norris, J.R., Thurnauer, M.C. and Griffin, R.G. (1993) Proc. Natl. Acad. Sci. USA 90, 9485–9488.
[20] Möbius, K. (1993) in: Biological Magnetic Resonance Vol. 13 (Berliner, L.J. and Reuben, J., Eds.) Plenum Press, New York, pp. 253–274.
[21] Morton, J.R. (1964) J. Am. Chem. Soc. 86, 2325–2329.
[22] Hales, B.J. (1975) J. Am. Chem. Soc. 97, 5993–5997.
[23] Lubitz, W., Broser, W., Kirste, B., Kurreck, H. and Schubert, K. (1978) Z. Naturforsch. 33a, 1072–1076.
[24] Kirste, B., Harrer, W., Kurreck, H., Schubert, K., Bauer, H. and Gierke, W. (1981) J. Am. Chem. Soc. 103, 6280–6286.
[25] Karplus, M. and Fraenkel, G.K. (1961) J. Chem. Phys. 35, 1312–1323.
[26] Atherton, N.M. (1993) Principles of Electron Spin Resonance, Ellis Horwood/PTR Prentice Hall, New York, London.
[27] Stehlik, D., Bock, C.H. and Petersen, J. (1989) J. Phys. Chem. 93, 1612–1619.
[28] Hore, P.J. (1990) in: Advanced EPR, Applications in Biology and Biochemistry (Hoff, A.J., Ed.) pp. 405–438, Elsevier, Amsterdam, New York.
[29] Van der Est, A., Bittl, R., Abresch, E.C., Lubitz, W., and Stehlik, D. (1993) Chem. Phys. Lett. 212, 561–568.
[30] Kleinfeld, D., Okamura, M.Y. and Feher, G. (1984) Biochem. 23, 5780–5786.
[31] Brzezinski, P., Okamura, M.Y. and Feher, G. (1992) in: The Photosynthetic Bacterial Reaction Center II (Breton, J. and Verméglio, A., Eds.) pp. 321–330, Plenum Press, New York.